

# MiR-96-5p is involved in permethrin-promoted proliferation and migration of breast cancer cells

Yi Yan, Tian Wen Long, Xi Niu, Jia Fu Wang and Sheng Li✉

Key Laboratory of Plant Resource Conservation and Germplasm Innovation in Mountainous Region (Ministry of Education), Collaborative Innovation Center for Mountain Ecology & Agro-Bioengineering, CICMEAB, College of Life Sciences/Institute of Agro-Bioengineering, Guizhou University, Guiyang 550025, Guizhou Province, China

**MicroRNAs (miRNAs) are major players in cellular responses to xenobiotic compounds and toxins. However, the role of miRNAs in pyrethroid pesticide-induced cancer progression remains unclear. This study aimed to investigate the function of miR-96-5p in permethrin-induced proliferation and migration in breast cancer cells. In our study, the expression of miR-96-5p was upregulated in permethrin-treated MCF-7 cells. MiR-96-5p promoted MCF-7 cell proliferation and migration, accompanied by changes in the expression of proteins involved in cell proliferation, migration, and apoptosis. Homeobox A5 (HOXA5) was identified as a direct target of miR-96-5p. HOXA5 silencing had the opposite effects with miR-96-5p inhibition. In conclusion, these results suggest that miR-96-5p is involved in permethrin-promoted proliferation and migration of breast cancer cells by targeting HOXA5.**

**Keywords:** miR-96-5p, permethrin, proliferation and migration, MCF-7 cells, HOXA5

**Received:** 23 October, 2022; **revised:** 16 November, 2022; **accepted:** 22 March, 2023; **available on-line:** 17 August, 2023

✉e-mail: [sl1@gzu.edu.cn](mailto:sl1@gzu.edu.cn)

**Acknowledgments of Financial Support:** This study was supported by the National Natural Science Foundation of China (No. 22166010 and No. 31401091).

**Abbreviations:** miRs, MicroRNAs; HOXA5, homeobox A5; CCK-8, Cell counting kit-8; 3'-UTR, 3'-untranslated regions; WT, Wild-type

## INTRODUCTION

Permethrin is a synthetic pyrethroid pesticide widely used in agriculture. Permethrin typically disturbs the nervous system of insects through slackening sensitivity toward voltage on the intramembrane and extramembrane of axons in the nervous system of insects (Park *et al.*, 2021; Wang *et al.*, 2016). Due to the efficient insecticidal properties of permethrin, it is not only applied to control crop diseases and pests but also used in mosquito killing and malaria treatment (Richards *et al.*, 2017; Richards *et al.*, 2018; Thievent *et al.*, 2019). However, the residual toxicity of permethrin has attracted great attention from the public. In vitro studies indicated that permethrin competitively combined with estrogen receptor (ER) against estradiol (E2) (McCarthy *et al.*, 2006) and promoted the proliferation of breast cancer cells, which could be blocked by estrogen antagonists (Kim *et al.*, 2004; Sun *et al.*, 2014). In addition, the wet weight of the uterus of female rats increased after being injected subcutaneously with permethrin, which was similar to the effect caused by E2, and permethrin-induced weight increase of the uterus could be inhibited by antiestrogenic

agents. When male mice were given permethrin *per os*, their luteinizing hormone (LH) significantly increased, while testosterone (T) level and sperm vitality dramatically decreased (Kim *et al.*, 2005). These studies indicate that pyrethroid pesticides such as permethrin have estrogenic effects and belong to environmental hormones. According to epidemiological observation, workers exposed to low-dose permethrin for a long time have higher risks of colorectal cancer, breast cancer, lung cancer, and leukemia (Rusiecki *et al.*, 2009). However, the underlying mechanisms remain elusive.

MicroRNA (miRNA) is a kind of non-coding small RNA and regulates protein expression by binding to the 3'-untranslated region (3'-UTR) of target genes (Burnett *et al.*, 2021; Cao *et al.*, 2021). miRNAs play an essential role in regulating the organismic response to toxic effects caused by xenobiotic compounds, including pesticides. For example, miR-22 restrained endothelial cell dysfunction caused by the pesticide endosulfan (Xu *et al.*, 2017). MiR-513 protected renal cells from DDVP-induced apoptosis by targeting BCL-2 (Li *et al.*, 2018). MiR-96-5p was initially identified as a 23-nucleotide miRNA and abundant evidence has shown that miR-96 is related to cell proliferation and apoptosis. For example, overexpression of miR-96-5p was shown to induce gastric adenocarcinoma cell apoptosis through targeting FOXO3 (He & Zou, 2020), and it also inhibited hepatocellular carcinoma cell apoptosis (Iwai *et al.*, 2018). MiR-96-5p inhibited the expression of the target gene MTSS1 and enhanced the growth of glioma cells (Zhang & Guo, 2019). These findings indicate that miR-96-5p is involved in tumor cell proliferation, migration, and apoptosis. However, the role of miR-96 in the cellular response to exogenous toxicants remains unclear.

HOXA5 is a member of homeobox gene clusters, which is involved in the regulation of cell differentiation. The role of HOXA5 in tumorigenesis is controversial. HOXA5 is generally regarded as a tumor suppressor in many cancers, such as cervical cancer and breast cancer. In these cancers, HOXA5 is normally the target of various miRNAs. On the other hand, HOXA5 is reported to be capable of promoting tumor progression, which needs further investigation.

Notably, the mechanism by which permethrin promotes breast cancer is not fully understood, and the role of miR-96-5p in breast cancer remains elusive. Therefore, in this study, we aimed to determine the regulatory role of miR-96-5p in mediating the estrogen effect of permethrin. Our study confirmed that miR-96-5p targeted HOXA5 to promote breast cancer induced by permethrin.

## MATERIALS AND METHODS

### Cell line and main reagents

MCF-7 cells were obtained from China Center for Type Culture Collection (CCTCC, China). Cell lines were cultured and maintained in Dulbecco's modified Eagle's medium (DMEM) (Gibco, USA) supplemented with 10% fetal bovine serum (FBS) (Gibco, USA), 1% penicillin and 1% streptomycin (both from Solarbio) under 5% CO<sub>2</sub> at 37°C. Permethrin standard (purity 99.1%) and 17β-estradiol standard (purity 99.2%) were purchased from China Center for Standard Substance; Trypsin was purchased from Sigma (USA); CCK-8 kit, Apoptosis-HOECHST staining kit, RNA Extracting Kit, PBS buffer, enhanced RIPA lysis buffer, BCA protein assay kit, and Lipo8000™ were purchased from Beyotime Technology (China). The primary and secondary antibodies were obtained from Beijing Quailiyard Biotechnology (China); U6 snRNA Real-time PCR Normalization Kit was purchased from Shanghai GenePharma (China).

### Cell proliferation assay

MCF-7 cells were seeded into 96-well plates at a density of  $3 \times 10^3$  cells/well. After overnight incubation, the cells reached about 70% confluency. Different concentrations of permethrin ( $10^{-4}$ ,  $10^{-5}$ ,  $10^{-6}$ ,  $10^{-7}$  mol/L) and estradiol ( $10^{-6}$ ,  $10^{-7}$ ,  $10^{-8}$ ,  $10^{-9}$  mol/L) were used to treat MCF-7 cells for 48 h or 72 h. Each treatment has five repeats and the medium with different drugs was refreshed daily. Cells untreated with drugs were set as the control group, and wells added only with the medium were set as the blank group. CCK-8 reagent allows the sensitive colorimetric assay to determine the number of viable cells in the cell proliferation assay. Therefore, 20 μL CCK-8 reagent was added to each well after different periods. After 30 min of incubation, the OD values of the solution in each well at 450 nm were measured to calculate cell viability according to the formula:

$$\text{Cell viability (\%)} = \frac{\text{OD}_{\text{treated group}} - \text{OD}_{\text{blank group}}}{\text{OD}_{\text{control group}} - \text{OD}_{\text{blank group}}} \times 100\%$$

### Cell transfection

MCF-7 cells were seeded into 6-well plates. After 70% confluency was reached, the cells in the control group were treated with 100 pmol scramble miRNA (marked as miR-NC group), while the cells in the experimental group were treated with 100 pmol miR-96-5p inhibitor or miR-96-5p mimic (marked as miR-96-5p inhibitor group or miR-96-5p mimic group) (GenePharma, China) using Lipofectamine 2000 (Invitrogen, USA). The medium was refreshed after 4 h, followed by 24 h incubation.

### Quantitative Real-time PCR

Total RNA was extracted with RNAeasy™ Animal RNA Isolation Kit and was reverse transcribed into cDNA using GenePharma RT Reagent Kit. The expression of miR-96-5p was measured with GenePharma qRT-PCR Kit. U6 snRNA was used as an internal reference for miRNA analysis. QRT-PCR was conducted using the CFX96 system. Primers were listed as follows: miR-96-5p, forward: 5'-CGAAGCTTTGGCACTAG-GCACATT-3', reverse: 5'-TATGGTTTTGACGACT-GTGTGAT-3'; U6, forward: 5'-CAGCACATATAC-

TAAAATTGGAACG-3', reverse: 5'-ACGAATTT-GCGTGTCCATCC-3'.

The relative expression of target genes was quantified using the  $2^{-\Delta\Delta Ct}$  method.

### Luciferase reporter assay

The targets of miR-96 were predicted by Target Scan Human (<http://www.targetscan.org>), miRDB (<http://mirdb.org>), and miRTarbase (<http://mirtarbase.mbc.nctu.edu.tw/php/index.php>). For the luciferase reporter assay, the wild-type (WT-*HOXA5*) or mutant 3'-untranslated regions (MUT-*HOXA5*) of *HOXA5* were subcloned into the luciferase reporter gene vector (pMIR-REPORTER Luciferase, cat. # QYV0423, Qualityyard, China). MCF-7 cells were cultured in 24-well plates, and co-transfected with miR-96-5p or miR-NC and WT-*HOXA5* or MUT-*HOXA5* plasmids using Lipofectamine 2000. The luciferase activity was calculated through the ratio of firefly and renilla luciferase activity following the manufacturer's instructions.

### In vitro wound healing assay

Cells were cultured in 12-well plates at a density of  $3 \times 10^5$  cells per well. After transfection with miR-NC, miR-96-5p mimic, and miR-96-5p inhibitor, cells were inoculated until 95% confluency was reached. A sterile 200-μL pipette tip was used to scratch the cell layer manually, and the time point was set as 0 h. Next, the cells were rinsed with PBS 3 times to remove all cellular debris. Fresh complete medium was then added. The subsequent colonization of the denuded surface was quantified with Image J, and the relative migration distance was calculated by subtracting the width at 0 h from the width at each migration time point.

### Western blot analysis

Cells were collected after 48 hours of transfection. Radio immuno-precipitation assay (RIPA) lysis buffer was used to extract total proteins and Bicinchoninic acid (BCA) protein assay kit was used to measure the concentrations of total proteins. Proteins of different molecular weights were separated by SDS-PAGE and transferred onto the membranes. After blocking with 5% skim milk for 1 h, proteins were incubated with primary antibodies, rabbit anti-*HOXA5*, and rabbit anti-β-actin at 4°C overnight. Subsequently, the membranes were washed with TBST solution, incubated with the secondary antibody goat anti-rabbit IgG coupled with HRP at room temperature for 2 h, and washed with TBST solution. The membranes were exposed using an ECL kit and Gel Imaging System. Each experiment was repeated 3 times.

### Statistical analysis

Data analysis, graph generation, and statistical analysis were performed with the software GraphPad Prism 8.3 (GraphPad Software Inc., Philadelphia, USA). Data were represented as mean ± standard deviation (S.D.). The comparison between the two groups was analyzed by *t*-test and the comparison of multiple groups such as different concentrations were analyzed by One-way analysis of variance (ANOVA). *P* values less than 0.05 were considered significant.

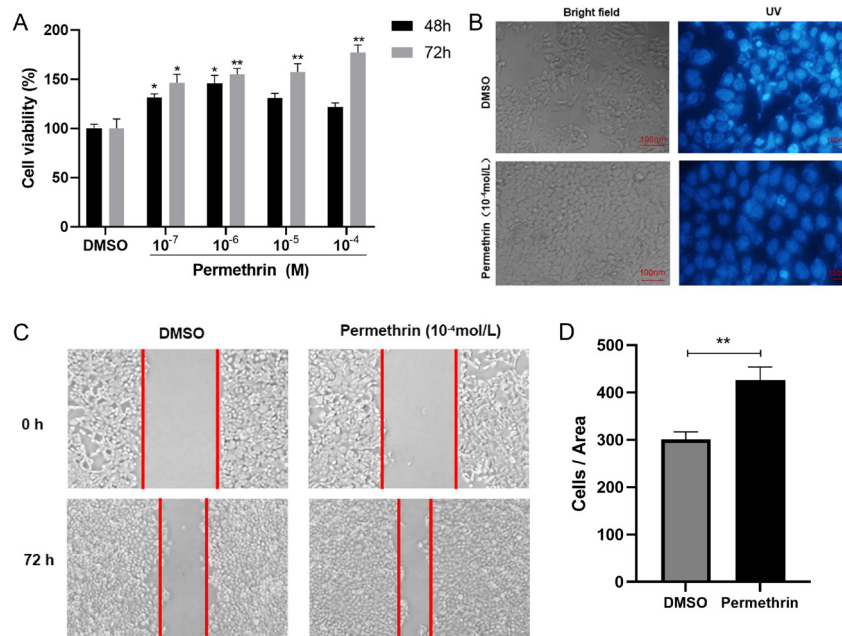


**Figure 1. Low-dose permethrin promoted the proliferation and migration of MCF-7 cells.**

(A) MCF-7 cells were treated with permethrin at different concentrations ( $10^{-4}$ – $10^{-7}$  M) for 48 or 72 h, and cell viability was assessed by CCK-8 assay. (B) Fluorescent microscopic images of Hoechst-stained MCF-7 cells after permethrin or control treatment. Bright blue fluorescence indicated apoptosis. (C) Wound of MCF-7 cells immediately after scratching and after 72 h culture in the control group and permethrin-treated group. (D) Statistical analysis of wound healing of MCF-7 cells. Data were mean  $\pm$  S.D. ( $n=3$ ). \* $P<0.05$ , \*\* $P<0.01$  versus NC groups.

## RESULTS

### Low-dose permethrin promoted the proliferation of MCF-7 cells

To determine the effect of permethrin on MCF-7 cell viability, the cells were treated with different concentrations of permethrin for 48 h or 72 h. The results showed that permethrin promoted MCF-7 cell proliferation in a dosage range from  $10^{-7}$  M to  $10^{-4}$  M (Fig. 1A). The maximum viability in MCF-7 cells was seen when cells were treated with  $10^{-4}$  M permethrin for 72 h. Hoechst staining showed that cells in treatment groups had higher viability. The nuclei were evenly stained, compared with the control group (Fig. 1B). IWH assay showed that MCF-7 cell migration was significantly promoted after treatment with  $10^{-4}$  M permethrin for 72 h (Fig. 1C). These results indicate that low-dose permethrin promotes MCF-7 cell proliferation and migration.

### Permethrin promoted ER- $\alpha$ and STAT3 expression and upregulated miR-96

Next, we investigated whether permethrin regulated the expression of genes involved in cell proliferation, employing estradiol as the positive control. As is shown in Fig. 2A, after treatment with low-dose estradiol and permethrin for 72 h, the expression of estrogen receptor- $\alpha$  (ER- $\alpha$ ) and Signal Transducer and Activator of Transcription (STAT3) in MCF-7 cells increased.

We performed a qRT-PCR assay to detect miR-96 expression in MCF-7 cells treated with different concentrations of permethrin. The results showed that miR-96 expression in MCF-7 cells in the permethrin-treated group increased in a dose-dependent manner (Fig. 2B).

### HOXA5 was a target of miR-96-5p in MCF-7 cells

HOXA5 gene was predicted to be the target of miR-96-5p by the TargetScan program (Fig. 3A). To verify the prediction, we constructed a luciferase reporter containing either the wild-type HOXA5 3' UTR or a mutated HOXA5 3' UTR and then co-transfected into

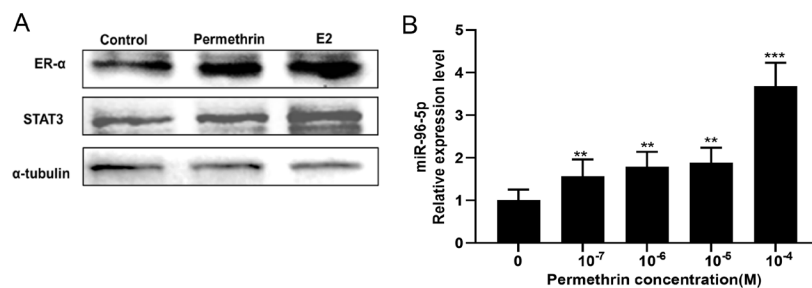


**Figure 2. Permethrin promoted ER- $\alpha$  and STAT3 expression and upregulated miR-96.**

(A) Western blot analysis of protein levels of ER- $\alpha$  and STAT3 in permethrin-treated MCF-7 cells. (B) PCR analysis of miR-96-5p levels in permethrin-treated MCF-7 cells. Data were mean  $\pm$  S.D. ( $n=3$ ). \* $P<0.05$ , \*\* $P<0.01$ , \*\*\* $P<0.001$  versus NC groups.

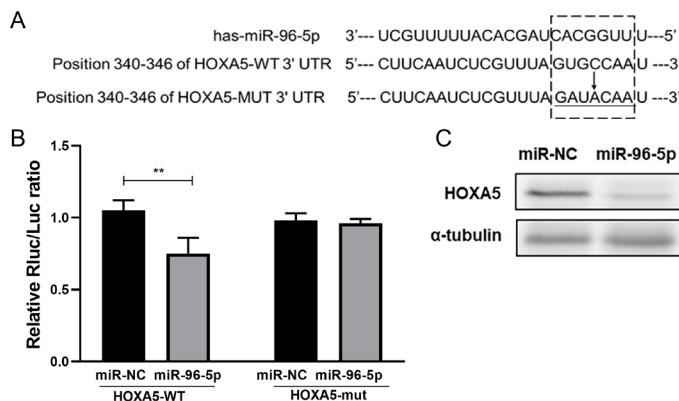


**Figure 3.** *HOXA5* is a target of miR-96-5p in MCF-7 cells.

(A) The predicted position of the miR-96-5p target site in the 3' UTR of *HOXA5*. The miR-96-5p seed sequence was shown in the box. (B) Luciferase report assay in cells co-transfected with *HOXA5* or *HOXA5* mutation reporter and miR-NC or miR-96-5p. (C) Western blot analysis of protein levels of *HOXA5* in miR-NC or miR-96-5p transfected MCF-7 cells. Data were mean  $\pm$  S.D. (n=3). \* $P$ <0.05, \*\* $P$ <0.01 versus NC groups.

MCF-7 cells with miR-96-5p mimic or negative control (NC) miRNAs. A significant decrease of luciferase activity was detected in cells co-transfected with *HOXA5* 3' UTR construct and miR-96-5p mimics, compared with cells co-transfected with miR-NC or mutant *HOXA5* 3' UTR (Fig. 3B). Compared with the miR-NC group, a significant decrease of *HOXA5* expression in miR-96-5p mimic group was observed (Fig. 3C). These results indicate that *HOXA5* is a direct target of miR-96-5p.

#### miR-96-5p promoted permethrin-induced proliferation and migration of MCF-7 cells by targeting *HOXA5*

To further investigate the mechanism of miR-96-5p in permethrin-induced MCF-7 cell proliferation and migration, the miR-96 inhibitor was transfected into permethrin-treated MCF-7 cells. IWH assay showed that permethrin-induced migration of MCF-7 cells was increased and *HOXA5* expression was upregulated after miR-96

was inhibited, compared with cells treated with permethrin only. In rescue experiments, permethrin-induced proliferation and migration of MCF-7 cells were decreased by silencing *HOXA5* expression (Fig. 4A, B, C). These results suggest that miR-96 regulates the proliferation and migration of MCF-7 cells by targeting *HOXA5*.

#### DISCUSSION

Estrogens are crucially involved in the development of breast cancer (Yi *et al.*, 2009; Chaudhuri *et al.*, 2021). Estrogen activates the ER dimer in the promoter domain of the target gene to regulate gene expression in cells (Krieg *et al.*, 2001). Estrogen also promotes the phosphorylation of related transcription factors (Sengupta *et al.*, 2019). Human breast cancer cell line MCF-7 is capable of expressing estrogen receptor and is sensitive to estrogen. Therefore, in the present study, we employed

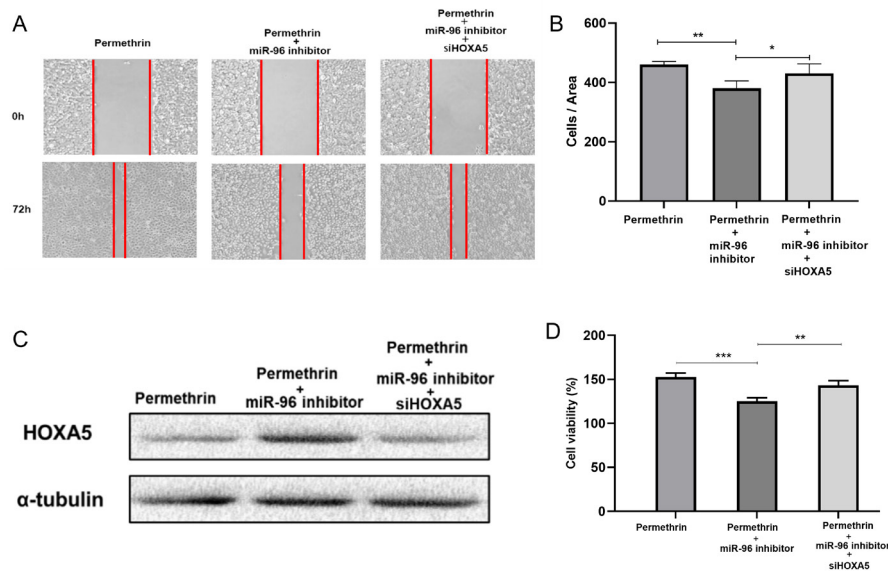


**Figure 4.** miR-96-5p promoted permethrin-induced proliferation and migration of MCF-7 cells through targeting *HOXA5*.

(A) Wound of permethrin-treated MCF-7 cells immediately after scratching and after 72 h culture in control or miR-96 inhibitor transfected group or miR-96 inhibitor/siHOXA5 co-transfected group. (B) Statistical analysis of wound healing of MCF-7 cells. (C) Western blot analysis of *HOXA5* expression after permethrin exposure in MCF-7 cells of the control group, transfected group, or co-transfected group. (D) Statistical analysis of the viability of MCF-7 cells in different groups. Data were mean  $\pm$  S.D. (n=3). \* $P$ <0.05, \*\* $P$ <0.01, \*\*\* $P$ <0.001 for the comparison.

the MCF-7 cell line as the experiment model and found that low-dose permethrin promoted the proliferation and migration of estrogen-sensitive MCF-7 cells. Moreover, we found that permethrin increased ER $\alpha$  protein expression as E2 did, indicating that permethrin plays a role in enhancing the metabolism of the estrogen receptor.

As a critical downstream transcription factor of ER, phosphorylated STAT3 passes through the nuclear pore to activate the transcription of target genes (Kettner *et al.*, 2019; Wang *et al.*, 2021). In our study, when MCF-7 cells were treated with low-dose permethrin, the expression of STAT3 and ER- $\alpha$  increased, compared with E2 treatment as the positive control. These results suggest that permethrin has an estrogen effect and promotes cell proliferation by activating the estrogen receptor and STAT-related estrogen pathway.

STAT3 is an important transcription factor of the miR-96-182-183 family (Lei *et al.*, 2021; Xiao *et al.*, 2021). MiR-96 was reported to influence the cell cycle (Xu *et al.*, 2018). miR-96 inhibitor arrested the cell cycle at the G1 phase, while fewer cells entered the S phase, suggesting that inhibition of miR-96 induces cell arrest in the G1 phase. Therefore, we speculated that miR-96 might promote cell proliferation and migration induced by permethrin. Our results showed that the miR-96 inhibitor attenuated permethrin-induced proliferation and migration of MCF-7 cells, which confirmed our speculation.

Next, TargetScan, miRDB, and miRTarbase were employed to predict the target genes of miR-96 (Guo *et al.*, 2021). *HOXA5* is highly correlated with cell proliferation and tumorigenesis. *HOXA5* is a member of the homeobox gene family encoding homologous proteins, and its biological function is to control embryonic development and cell differentiation. *HOXA5* is regulated by AKT/mTORC1/S6K1 signal pathway (Feng *et al.*, 2017), and inhibits cell progression by regulating AKT/p27 pathway (Wang *et al.*, 2019). *HOXA5* expression was closely related to tumor histological grade (Dziobek *et al.*, 2020; Aubin *et al.*, 2002). Inhibition and overexpression of *HOXA5* promoted proliferation and apoptosis of osteosarcoma cells through the p53 and p38 $\alpha$ /MAPK pathways (Chen *et al.*, 2019). Inhibition of *HOXA5* significantly enhanced viability and proliferation in U2OS and MG63 cells, while overexpression of *HOXA5* promoted cell apoptosis and caspase-3 activity. Knockdown of *HOXA5* in HCC cells provoked capillary tube formation, while overexpression of *HOXA5* inhibited cell proliferation and invasion and promoted cell apoptosis. Based on the luciferase assay, we confirmed that *HOXA5* was a target gene of miR-96. When *HOXA5* was overexpressed, proliferation and migration in MCF-7 cells induced by permethrin were inhibited. Therefore, overexpression of *HOXA5* could reverse the effects of miR-96. These results suggest that miR-96 promotes permethrin-induced proliferation and migration in MCF-7 cells via the downregulation of *HOXA5*. A recent study reported the potential of miRNAs as biomarkers of breast cancer (Shaaban *et al.*, 2022). It would be interesting to evaluate the application of miR-96 in the early diagnosis of breast cancer.

This study has certain limitations. First, the downstream mechanism of Permethrin, miR-96-5p, and *HOXA5* in promoting breast cancer is still obscure. In addition, we need to perform *in vivo* experiments to confirm our conclusion in future studies. Beyond these limitations, this is the first study to demonstrate that miR-96-5p targeted *HOXA5* to promote cancer progression.

In conclusion, our results suggest that permethrin, as a pseudo estrogen, upregulates ER- $\alpha$  and STAT3 expres-

sion in MCF-7 cells. STAT3 activates the transcription of miR-96, which specifically inhibits *HOXA5* expression and promotes the proliferation and migration of MCF-7 cells.

### Conflict of Interest

The authors declare that there are no conflicts of interest.

### REFERENCES

- Aubin J, Dery U, Lemieux M, Chailier P, Jeannotte L (2002) Stomach regional specification requires *HOXA5*-driven mesenchymal-epithelial signaling. *Development* **129**: 4075–4087. <https://doi.org/10.1242/dev.129.17.4075>
- Burnett M, Rodolico V, Shen F, Leng R, Zhang M, Eisenstat D D, Serge C (2021) PathVisio Analysis: An application targeting the miRNA network associated with the p53 signaling pathway in osteosarcoma. *BioCell* **45**: 17–26
- Cao L, Yang DM, Bai B. (2021) Mir-1247 Affects the proliferation, invasion and apoptosis of osteosarcoma cells through SOX9. *Oncology* **23**: 149–158
- Chaudhuri S, Thomas S, Munster P. (2021) Immunotherapy in breast cancer: A clinician's perspective. *J Natl Cancer Center* **1**: 47
- Chen YQ, Yang TQ, Zhou B, Yang MX, Feng HJ, Wang YL (2019) *HOXA5* overexpression promotes osteosarcoma cell apoptosis through the p53 and p38 $\alpha$  MAPK pathway. *Gene* **689**: 18–23. <https://doi.org/10.1016/j.gene.2018.11.081>
- Dziobek K, Oplawski M, Zmarzly N, Gabarek BO, Kielbasinski R, Kielbasinski K, Kieszkowski P, Talkowski K, Boron D (2020) Assessment of expression of homeobox A5 in endometrial cancer on the mRNA and protein level. *Curr Pharm Biotechnol* **21**: 635–641. <https://doi.org/10.2174/1389201021666191227121627>
- Feng F, Ren Q, Wu S, Saeed M, Sun C (2017) *HOXA5* increases mitochondrial apoptosis by inhibiting Akt/mTORC1/S6K1 pathway in mice white adipocytes. *Oncotarget* **8**: 95332–95345. <https://doi.org/10.18632/oncotarget.20521>
- Guo Q, Yuan Y, Zhang X, Lei X, Yuan Q, Li H (2021) miR-181a-3p inhibits malignant biological behavior of non-small cell lung cancer via down-regulating RAD21 expression. *J Comp Mol Sci Genet* **2**: 12–23
- He X, Zou K (2020) MiRNA-96-5p contributed to the proliferation of gastric cancer cells by targeting FOXO3. *J Biochem* **167**: 101–108. <https://doi.org/10.1093/jb/mvz080>
- Iwai N, Yasui K, Tomie A, Gen Y, Terasaki K, Kitaichi T, Soda T, Yamada N, Dohi O, Seko Y, Umemura A, Nishikawa T, Yamaguchi K, Moriguchi M, Konishi H, Naito Y, Itoh Y (2018) Oncogenic miR-96-5p inhibits apoptosis by targeting the caspase-9 gene in hepatocellular carcinoma. *Int J Oncol* **53**: 237–245. <https://doi.org/10.3892/ijo.2018.4369>
- Kettner NM, Vijayaraghavan S, Durak MG, Bui T, Kohansal M, Ha MJ, Liu B, Rao X, Wang J, Yi M, Carey JPW, Chen X, Eckols TK, Raghavendra AS, Ibrahim NK, Karuturi MS, Watowich SS, Sahin A, Tweardy DJ, Hunt KK, Tripathy D, Keyomarsi K (2019) Combined inhibition of STAT3 and DNA repair in palbociclib-resistant ER-positive breast cancer. *Clin Cancer Res* **25**: 3996–4013. <https://doi.org/10.1158/1078-0432.CCR-18-3274>
- Kim IY, Shin JH, Kim HS, Lee SJ, Kang IH, Kim TS, Moon HJ, Choi KS, Moon A, Han SY (2004) Assessing estrogenic activity of pyrethroid insecticides using *in vitro* combination assays. *J Reprod Dev* **50**: 245–255. <https://doi.org/10.1262/jrd.50.245>
- Kim SS, Lee RD, Lim KJ, Kwack SJ, Rhee GS, Seok JH, Lee GS, An BS, Jeung EB, Park KL (2005) Potential estrogenic and antiandrogenic effects of permethrin in rats. *J Reprod Dev* **51**: 201–210. <https://doi.org/10.1262/jrd.16060>
- Krieg SA, Krieg AJ, Shapiro DJ (2001) A unique downstream estrogen responsive unit mediates estrogen induction of proteinase inhibitor-9, a cellular inhibitor of IL-1 $\beta$ -converting enzyme (caspase 1). *Mol Endocrinol* **15**: 1971–1982. <https://doi.org/10.1210/mend.15.11.0719>
- Lei H, Shi J, Teng Y, Song C, Zou L, Ye F, Zhang H (2021) Baicalin modulates the radiosensitivity of cervical cancer cells *in vitro* via miR-183 and the JAK2/STAT3 signaling pathway. *Adv Clin Exp Med* **30**: 727–736. <https://doi.org/10.17219/acem/135478>
- Li S, Xu YN, Niu X, Li Z, Wang JF (2018) miR-513a-5p targets Bcl-2 to promote dichlorvos induced apoptosis in HK-2 cells. *Biomol Pharm* **108**: 876–882. <https://doi.org/10.1016/j.biopha.2018.09.101>
- McCarthy AR, Thomson BM, Shaw IC, Abell AD (2006) Estrogenicity of pyrethroid insecticide metabolites. *J Environ Monit* **8**: 197–202. <https://doi.org/10.1039/b511209e>
- Park SK, Lee HJ, Song E, Kim Y, Kim DY, Lee JH, Yoo HJ, Oh JE, Kwon JH (2021) Exposure to permethrin used as a home in-

- secticide: A case study comparing model predictions and excretion of metabolites. *Environ Int* **155**: 106581. <https://doi.org/10.1016/j.envint.2021.106581>
- Richards SL, Balanay JAG, Harris JW, Banks VM, Meshnick S (2017) Residual effectiveness of permethrin-treated clothing for prevention of mosquito bites under simulated conditions. *J Environ Health* **79**: 8–15
- Richards SL, Agada N, Balanay JAG, White AV (2018) Permethrin treated clothing to protect outdoor workers: evaluation of different methods for mosquito exposure against populations with differing resistance status. *Pathog Glob Health* **112**: 13–21. <https://doi.org/10.1080/20477724.2018.1437692>
- Rusiecki JA, Patel R, Koutros S, Beane-Freeman L, Landgren O, Bonner MR, Coble J, Lubin J, Blair A, Hoppin JA, Alavanja MC (2009) Cancer incidence among pesticide applicators exposed to permethrin in the Agricultural Health Study. *Environ Health Perspect* **117**: 581–586. <https://doi.org/10.1289/ehp.11318>
- Sengupta S, Sevigny CM, Bhattacharya P, Jordan VC, Clarke R (2019) Estrogen-induced apoptosis in breast cancers is phenocopied by blocking dephosphorylation of eukaryotic initiation factor 2 Alpha (eIF2alpha) protein. *Mol Cancer Res* **17**: 918–928. <https://doi.org/10.1158/1541-7786.MCR-18-0481>
- Shaaban NZ, Ibrahim NK, Saada HN, El-Rashidy FH, Shaaban HM (2022). The Implication of microRNAs as non-invasive biomarkers in 179 Egyptian breast cancer female patients. *Oncol Res* **30**: 269–276
- Sun H, Chen W, Xu X, Ding Z, Chen X, Wang X (2014) Pyrethroid and their metabolite, 3-phenoxybenzoic acid showed similar (anti)estrogenic activity in human and rat estrogen receptor alpha-mediated reporter gene assays. *Environ Toxicol Pharmacol* **37**: 371–377. <https://doi.org/10.1016/j.etap.2013.11.031>
- Thievent K, Hauser G, Elaïan O, Koella JC (2019) The interaction between permethrin exposure and malaria infection affects the host-seeking behaviour of mosquitoes. *Malar J* **18**: 79. <https://doi.org/10.1186/s12936-019-2718-x>
- Wang X, Martinez MA, Dai M, Chen D, Ares I, Romero A, Castellano V, Martinez M, Rodriguez JL, Martinez-Larranaga MR, Anadon A, Yuan Z (2016) Permethrin-induced oxidative stress and toxicity and metabolism. A review. *Environ Res* **149**: 86–104. <https://doi.org/10.1016/j.envres.2016.05.003>
- Wang Y, Duan Y, Chen K, Li H, Quan Y. (2021) Protective effects of docosahexaenoic acid against non-alcoholic hepatic steatosis through activating of JAK2/STAT3 signaling pathway. *Biocell* **45**: 307–316
- Wang Z, Yu C, Wang H (2019) *HOXA5* inhibits the proliferation and induces the apoptosis of cervical cancer cells *via* regulation of protein kinase B and p27. *Oncol Rep* **41**: 1122–1130. <https://doi.org/10.3892/or.2018.6874>
- Xiao Y, Huang W, Huang H, Wang L, Wang M, Zhang T, Fang X, Xia X (2021) miR-182-5p and miR-96-5p target PIAS1 and mediate the negative feedback regulatory loop between PIAS1 and STAT3 in endometrial cancer. *DNA Cell Biol* **40**: 618–628. <https://doi.org/10.1089/dna.2020.6379>
- Xu D, Guo Y, Liu T, Li S, Sun Y (2017) miR-22 contributes to endosulfan-induced endothelial dysfunction by targeting SRF in HUVECs. *Toxicol Lett* **269**: 33–40. <https://doi.org/10.1016/j.toxlet.2017.01.014>
- Xu T, Du XW, Hu JB, Zhu YF, Wu HL, Dai GP, Shu YM, Ouyang J (2018) Anticancer effect of miR-96 inhibitor in bladder cancer cell lines. *Oncol Lett* **15**: 3814–3819. <https://doi.org/10.3892/ol.2018.7745>
- Yi JM, Kwon HY, Cho JY, Lee YJ (2009) Estrogen and hypoxia regulate estrogen receptor alpha in a synergistic manner. *Biochem Biophys Res Commun* **378**: 842–846. <https://doi.org/10.1016/j.bbrc.2008.11.142>
- Zhang S, Guo W (2019) Long noncoding RNA MEG3 suppresses the growth of glioma cells by regulating the miR965p/MTSS1 signaling pathway. *Mol Med Rep* **20**: 4215–4225. <https://doi.org/10.3892/mmr.2019.10659>